Thermal stability of Co-core-CoO-shell nanoparticles on an ultrathin θ–Al_2O_3 film support

V. Rose, and R. Franchy

Citation: Journal of Applied Physics **101**, 086104 (2007);
View online: https://doi.org/10.1063/1.2717127
View Table of Contents: http://aip.scitation.org/toc/jap/101/8
Published by the American Institute of Physics

Thermal stability of Co-core-CoO-shell nanoparticles on an ultrathin θ-Al_2O_3 film support

V. Rose[a)]
Center for Nanoscale Materials and Advanced Photon Source, Argonne National Laboratory, Argonne, Illinois 60439

R. Franchy[b)]
Institute for Surfaces and Interfaces (ISG 3), Research Center Jülich, 52425 Jülich, Germany

(Received 30 January 2007; accepted 5 February 2007; published online 20 April 2007)

The effect of annealing temperature on a system of Co-core-CoO-shell nanoparticles on θ-Al_2O_3/CoAl(100) has been investigated using a combination of Auger electron spectroscopy, high-resolution electron energy loss spectroscopy, low-energy electron diffraction, and scanning tunneling microscopy. Results show that thermal treatment leads to a decomposition of the CoO-shell above 450 K, and thus it is strongly diminished with respect to the bulk value. Between 550 and 1050 K the Co particles coalescence and diffuse through the oxide into the substrate. Due to defect recovery, the thermal stability of the thin aluminum oxide film remained unchanged compared to as-grown θ-Al_2O_3. © *2007 American Institute of Physics*. [DOI: 10.1063/1.2717127]

Magnetic nanoparticles play a central role in various scientific fields and technological applications such as heterogeneous catalysis, medicine, and magnetic data storage devices.[1–3] In particular, nanoparticles that contain an interface between a ferromagnetic core and an antiferromagnetic shell, such as Co-core-CoO-shell particles,[4–7] are of vital importance. When such particles are cooled in a magnetic field, they may exhibit an additional unidirectional anisotropy due to magnetic coupling at the interface, also referred to as exchange biasing, that leads to magnetization stability.[8,9] Exchange-biased nanoparticles could open the path to significant technological applications associated with further miniaturization of devices,[10] because they overcome the so-called superparamagnetic limit[11] that occurs when the magnetic anisotropy energy per particle becomes comparable to the thermal energy. Many spintronic applications, such as advanced magnetic-based sensors and random-access memories, further rely on nanoparticles supported on thin oxide films being stable under thermal treatment.[12,13] Consequently, the understanding of the thermal stability of nanoparticles on oxide supports is of fundamental interest.

In this work we present Auger electron spectroscopy (AES), scanning tunneling microscopy (STM), low energy electron diffraction (LEED), and electron energy loss spectroscopy (EELS) measurements of the thermal treatment of Co-core-CoO-shell nanoparticles on θ-Al_2O_3 grown on CoAl(100). Results show that decomposition of the CoO shell sets in at 450 K, followed by coalescence and diffusion of Co through the oxide into the CoAl substrate at elevated temperatures. The thermal stability and structure of the thin aluminum oxide support remain unaffected compared to as-grown θ-Al_2O_3.

The experiments reported were performed in two separate ultrahigh vacuum (UHV) systems with base pressures better than 1×10^{-10} mbar. The first chamber was equipped with a cylindrical mirror analyzer (CMA) for AES, a three-grid optic for LEED, and an EEL spectrometer. The surface sensitivity of AES was improved by decreasing the incidence angle of a second electron gun to 3° (GIAES) in addition to a conventional normal incidence electron gun (NIAES) using the same CMA. Utilization of the two methods of AES allows us to distinguish between Auger electrons from elements either embedded far from or near the sample surface. The EEL spectra were taken in specular geometry and at the primary energy of 4 eV. A second UHV chamber was used to record STM images in the constant current mode utilizing chemically etched tungsten tips. It was also equipped with facilities for AES and LEED.

After cleaning of the CoAl(100) surface by repeated cycles of Ar^+ ion sputtering and subsequent annealing under UHV by electron bombardment, a 0.9-nm-thick θ-Al_2O_3 support was grown via selective segregation epitaxy of CoAl(100), in which only one metallic component of the intermetallic alloy is oxidized.[14] The well-ordered alumina surface exhibits a streak structure, composed of elongated islands with lengths up to around 100 nm that grow in two sets of domains perpendicular to each other. Nominal 3 nm Co was then deposited on θ-Al_2O_3/CoAl(100) at 300 K from a water-cooled evaporator using electron bombardment of a Co rod with a deposition rate of 0.1 nm/min. Cobalt exhibits a three-dimensional growth mode in agreement with thermodynamic considerations. A thin CoO shell was naturally formed due to a surfactant effect of oxygen on the growth of Co nanoparticles.[15] In all experiments, each annealing temperature T_{heat} was held constant for 2 min and the sample was then allowed to cool down to 300 K before performing the measurements.

In Fig. 1, we present NIAES and GIAES measurements of the peak-to-peak ratio of O_{KLL} (503 eV)/Co_{LMM} (775 eV)

[a)]Author to whom correspondence should be addressed; electronic mail: vrose@anl.gov
[b)]Deceased.

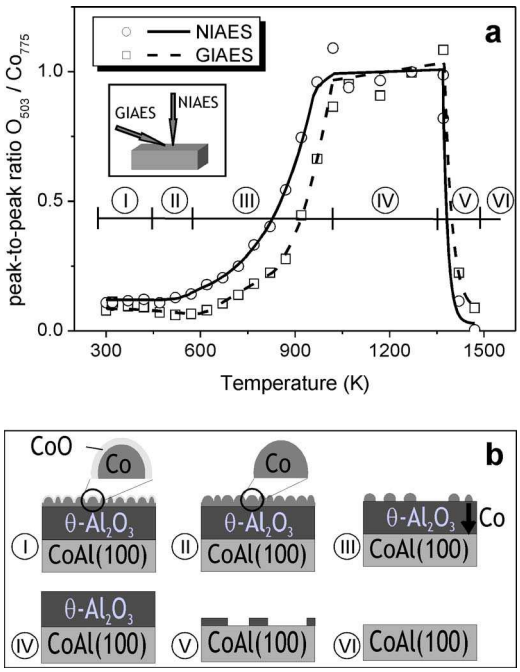

FIG. 1. (a) Normalized peak-to-peak ratio of the O_{KLL} (503 eV) and Co_{LMM} (775 eV) AES transitions of Co-core-CoO-shell particles on θ-Al_2O_3/CoAl(100) as a function of annealing temperature, measured with a normal incidence (NIAES) and grazing incidence (GIAES) primary electron gun. The nominal Co coverage amounts to 3 nm. (b) Corresponding schematic representations of the sample for the characteristic temperature regions (I–VI).

of the Cobalt-core-CoO-shell/θ-Al_2O_3/CoAl(100) sample as a function of T_{heat}. Six characteristic T_{heat} regions (I–VI) can be deduced from the data as discussed in the following. Corresponding schematic representations of the sample are shown in Fig. 1(b). Up to T_{heat}=450 K (cf. I), the Co-core-CoO-shell nanoparticles are stable, indicated by a constant O/Co ratio in both GIAES and NIAES. Because GIAES predominantly probes the oxygen signal from the CoO shell and not the underlying alumina,[15] the drop of the O/Co ratio for T_{heat} between 450 and 550 K (cf. II) can be assigned to the decomposition of the thin CoO shell. The melting point of bulk CoO is considerably higher and amounts to 2208 K.[16] Further annealing between 550 and 1050 K (cf. III) leads to a drastic increase of the Co/O ratio in both the GIAES and NIAES geometry, induced by the diffusion of Co through the oxide into the CoAl(100) substrate. The O/Co ratio then reaches a plateau for T_{heat} of 1050–1300 K (cf. IV). This region characterizes the thermal stability of the Al_2O_3 support. The same stability was also found for a clean as-prepared Al_2O_3 film on CoAl(100),[14] which suggests that the diffusion process of Co is accompanied by a defect recovery in the oxide film. The decrease of the Co/O ratio for T_{heat} of 1300–1450 K (cf. V) describes the decomposition of the alumina film. Finally, for $T_{heat}>1450$ the thermal treatment yields a clean CoAl(100) surface. In the case of Co clusters on γ-Al_2O_3 on Ni_3Al, diffusion through the oxide film into the substrate was found at 700 K, which is comparable to our results.[17] However, thermal stability for Co clusters on Al_2O_3/NiAl(100) was reported even between 800 and 1090 K,[18] which evinces the influence of the oxide phase onto the

TABLE I. Overview of the characteristic annealing temperatures T_{heat} that correspond to the different stages of the thermal stability of the Co-core-CoO-shell/θ-Al_2O_3/CoAl(100) system. The schematic representations are shown in Fig. 1(b).

	T_{heat} (K)	Description
I	300–450	Sample thermally stable
II	450–550	CoO decomposition
III	550–1050	Co diffusion
IV	1050–1300	Al_2O_3 thermally stable
V	1300–1450	Al_2O_3 decomposition
VI	>1450	Clean CoAl(100)

thermal stability of Co particles. An overview of the different thermal stability ranges found during annealing of Co-core-CoO-shell nanoparticles on θ-Al_2O_3 grown on CoAl(100) is shown in Table I.

The decomposition of CoO and the thermal stability of Co were also studied with EELS. After the annealing at 320 K, the EEL spectrum exhibits a broad loss structure at 350 −580 cm^{-1} (Fig. 2). This feature originates from the convolution of the characteristic Fuchs–Kliewer mode (535 cm^{-1}) and the $^4E \leftarrow {}^4A_2$ energy transition (410 cm^{-1}) of CoO.[15] After annealing at 520 K, the spectrum shows for the first time previously screened modes of the well-ordered alumina support (430, 630, and 920 cm^{-1}) in superimposition with the CoO modes. Further annealing leads to diffusion of Co through the oxide and thus, an increase of the intensity of the Al_2O_3 modes, while the CoO losses are vanished (cf. 720 K). After annealing at 1020 K the EEL spectrum corresponds to a well-ordered oxide film.

Utilizing LEED, no long-range order is visible on the entirely Co-covered oxide film after deposition at 300 K.[15] First weak Bragg reflections of the oxide support are observable after annealing at 700 K indicating isolated uncovered

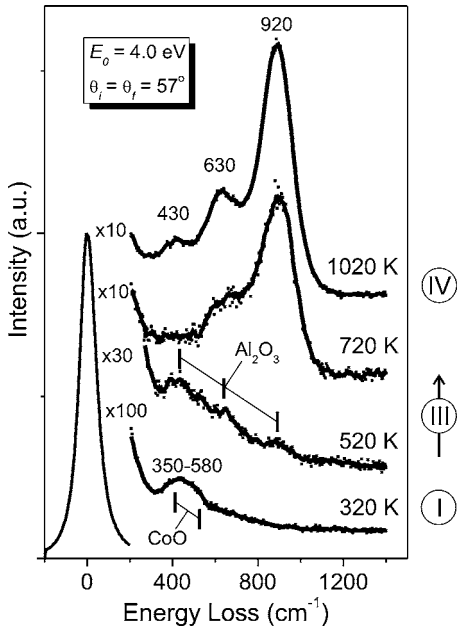

FIG. 2. Set of EELS spectra (E_0=4 eV) of the annealing of Co-core-CoO-shell nanoparticles on θ-Al_2O_3/CoAl(100). At 320 K, the spectrum exhibits only the modes of CoO. With increasing annealing temperature the CoO losses vanish and the modes of the Al_2O_3 support show up.

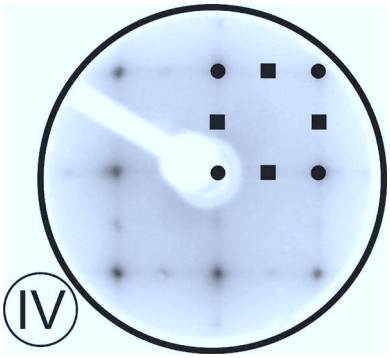

FIG. 3. The reappearing (2×1) LEED pattern (E_p=70 eV) of the θ-Al_2O_3/CoAl(100) support after annealing at 1020 K. Some reflexes are marked for better understanding.

oxide surface regions. Further annealing leads to an increase of the intensity of the Bragg reflections and a decrease of the diffuse background. After annealing at 1020 K, the (2×1) LEED pattern of the θ-Al_2O_3 film is clearly visible (cf. Fig. 3).

Figure 4 shows STM images with a scanned area of 75 $\times$75 nm^2 illustrating thermal stability of Co-core-CoO-shell nanoparticles on θ-Al_2O_3 grown on CoAl(100). Due to experimental reasons, we had to remove the scanning tunneling microscope from the sample. Thus, every STM image represents a different area of the sample surface, but the morphology shown is indicative of the entire surface. After deposition, spherical cobalt-core-CoO-shell particles with a mean diameter d_m=3 nm are observed [Fig. 4(a)]. The particles tend to form chains, as predetermined by the streak structure of the oxide template. After annealing at 500 K [Fig. 4(b)], d_m decreases to 2.6 nm, which can be assigned to the decomposition of the CoO shell of the Co particles. The mean thickness of the CoO shell can be estimated to be around 0.2 nm. For further annealing, two effects can be simultaneously observed on the surface: First, the Co particles start to coalescence, and second, Co diffuses through the oxide into the substrate. After annealing at 700 K [Fig. 4(c)], particles with d_m=4.5 nm are present. The dark contrast shows an uncovered region of the alumina film close to an oxide step edge,

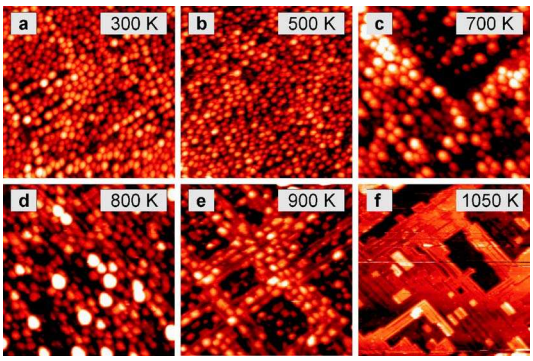

FIG. 4. (Color online) Set of STM images (75$\times$75 nm^2) of the annealing of the system Co-core-CoO-shell/θ-Al_2O_3/CoAl(100) taken after (a) deposition at 300 K, (b) annealing at 500, (c) 700, (d) 800, (e) 900, and (f) 1050 K.

in agreement with the first appearance of the oxide LEED pattern. While after annealing at 800 K [Fig. 4(d)] some large particles appear as bright contrasts, the majority now tends to form elongated and rectangular shapes with reduced size. After annealing at 900 K [Fig. 4(e)], it becomes obvious that the edges of the rectangular Co particles are parallel to the domains of the oxide support, indicating a strong interaction between the Co particles and the θ-Al_2O_3 support. After annealing at 1050 K, Co is entirely removed from the surface and the oxide exhibits the characteristic streak structure.

In summary, Co-core-CoO-shell nanoparticles are stable on θ-Al_2O_3 up to an elevated temperature of 450 K. However, the thermal stability of the CoO shell is strongly diminished with respect to the bulk value. The STM data suggest that the naturally formed CoO shell is only 0.2 nm thick. Annealing above 450 K leads to a decomposition of the CoO shell, followed by coalescence of Co particles and a diffusion of Co into the substrate. Notably, the Co diffusion process does not alter the thermal stability of the well-ordered oxide template.

The project has been completed at Research Center Jülich with kindly support of Prof. Harald Ibach. The late René Franchy (see Ref. 19) is acknowledged for the contributions to the research for this article. Work at Argonne is supported by the U.S. Department of Energy, Office of Sciences, Office of Basic Energy Sciences, under Contract No. DE-AC02–06CH11357.

[1] H.-J. Freund, Surf. Sci. **500**, 271 (2002).
[2] R. H. Kodama, J. Magn. Magn. Mater. **200**, 359 (1999).
[3] *Scientific and Clinical Applications of Magnetic Materials*, edited by U. Häfeli, W. Schütt, J. Teller, and M. Zborowski (Plenum, New York, 1997).
[4] J. B. Tracy, D. N. Weiss, D. P. Dinega, and M. G. Bawendi, Phys. Rev. B **72**, 064404 (2005).
[5] C. Portemont, R. Morel, A. Brenac, and L. Notin, J. Appl. Phys. **100**, 033907 (2006).
[6] J. Nogués, V. Skumryev, J. Sort, S. Stoyanov, and D. Givord, Phys. Rev. Lett. **97**, 157203 (2006).
[7] J. B. Tracy and M. G. Bawendi, Phys. Rev. B **74**, 184434 (2006).
[8] A. E. Berkowitz and K. Takano, J. Magn. Magn. Mater. **200**, 552 (1999).
[9] V. Skumryev, S. Stoyanov, Y. Zhang, G. Hadjipanayis, D. Givord, and J. Nogués, Nature (London) **423**, 850 (2003).
[10] J. Nogués, J. Sort, V. Langlais, V. Skumryev, S. Suriñach, J. S. Muños, and M. D. Baró, Phys. Rep. **422**, 65 (2005).
[11] D. Weller and A. Moser, IEEE Trans. Magn. **35**, 4423 (1999).
[12] U. Hartmann and R. Cochoorn, *Magnetic Multilayers and Giant Magnetoresistance: Fundamentals and Industrial Applications* (Springer, Berlin, 2000).
[13] *Spin Dependent Transport in Magnetic Nanostructures*, edited by S. Maekawa and T. Shinjo (Taylor & Francis, London, 2002).
[14] V. Rose, V. Podgursky, I. Costina, R. Franchy, and H. Ibach, Surf. Sci. **577**, 139 (2005).
[15] V. Rose, V. Podgursky, R. David, and R. Franchy, Surf. Sci. **601**, 786 (2007).
[16] J. A. Young, J. Chem. Educ. **78**, 1328 (2001).
[17] V. Podgursky, I. Costina, and R. Franchy, Surf. Sci. **529**, 419 (2003).
[18] W. C. Lin, S. S. Wong, P. C. Huang, C. B. Wu, B. R. Xu, C. T. Chiang, H. Y. Yen, and M. T. Lin, Appl. Phys. Lett. **89**, 153111 (2006).
[19] H. Ibach, T. Raman, A. Otto, L. Baker, and B. Frederick, Surf. Sci. **587**, XV (2005).